

AD-A102 775

JOINT INST FOR LAB ASTROPHYSICS BOULDER CO  
MEASUREMENT OF ELECTRON EXCITATION OF THE A 1 DELTA G STATE OF --ETC(U)  
MAY 81 K TACHIBANA, A V PHELPS MIPR-FY1455-80-00607

F/G 7/2

NI

UNCLASSIFIED

AFWAL-TR-81-2038

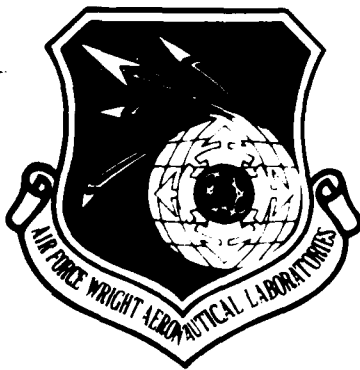
1 of 1  
40A  
00775

END  
DATE FILMED  
9-81  
DTIC

AD A102775

REF ID: AFWAL-TR-81-2038

12



MEASUREMENT OF ELECTRON EXCITATION OF THE  $a^1 \Delta_g$  STATE OF O<sub>2</sub>  
USING THE SWARM TECHNIQUE

K. TACHIBANA AND A. V. PHELPS

QUANTUM PHYSICS DIVISION  
U.S. BUREAU OF STANDARDS  
BOULDER, CO 80303

MAY 1981

FINAL REPORT FOR PERIOD OCTOBER 1979 - SEPTEMBER 1980

DTIC  
AUG 13 1981

DTIC FILE COPY

Approved for public release; distribution unlimited

AERO PROPULSION LABORATORY  
AIR FORCE WRIGHT AERONAUTICAL LABORATORIES  
AIR FORCE SYSTEMS COMMAND  
WRIGHT-PATTERSON AIR FORCE BASE, OHIO 45433

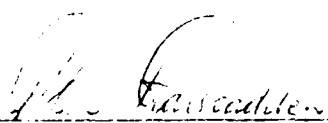
818 13 003

NOTICE

When Government drawings, specifications, or other data are used for any purpose other than in connection with a definitely related Government procurement operation, the United States Government thereby incurs no responsibility nor any obligation whatsoever; and the fact that the Government may have formulated, furnished, or in any way supplied the said drawings, specifications, or other data, is not to be construed by implication or otherwise as in any manner licensing the holder or any other person or corporation, or conveying any rights or permission to manufacture, use, or sell any patented invention that may in any way be related thereto.

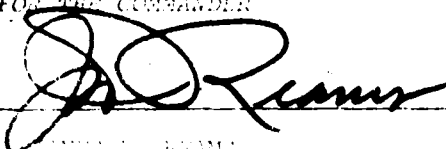
This report has been reviewed by the Office of Public Affairs (ASD/PA) and is releasable to the National Technical Information Service (NTIS). At NTIS, it will be available to the general public, including foreign nations.

This technical report has been reviewed and is approved for publication.

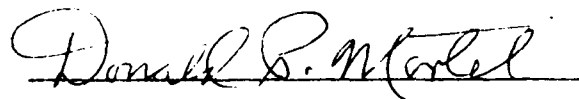


J. H. HARROLD  
LABORATORY ENGINEER

FOR THE COMMANDER



DONALD P. MORREL  
Acting Chief, Energy Conversion Branch  
Aerospace Power Division  
Aero Propulsion Laboratory



DONALD P. MORREL  
Acting Chief, Energy Conversion Branch  
Aerospace Power Division  
Aero Propulsion Laboratory

"If your address has changed, if you wish to be removed from our mailing list, or if the addressee is no longer employed by your organization please notify AFWAL/POOC X-PAFB, OH 45433 to help us maintain a current mailing list".

Copies of this report should not be returned unless return is required by security considerations, contractual obligations, or notice on a specific document.

REPORT DOCUMENTATION PAGE		READ INSTRUCTIONS BEFORE COMPLETING FORM
1. REPORT NUMBER AFWAL-TR-81-2038	2. GOVT ACCESSION NO. <i>AD-A102</i>	3. RECIPIENT'S CATALOG NUMBER <i>775</i>
4. TITLE (and Subtitle) Measurement of Electron Excitation of the $\alpha^1 A_g$ State of $O_2$ Using the Swarm Technique		5. TYPE OF REPORT & PERIOD COVERED Final Oct. 79 - Sept. 80
7. AUTHOR(s) K. Tachibana and A. V. Phelps	6. PERFORMING ORG. REPORT NUMBER MIPR FY1455-80-00607	
9. PERFORMING ORGANIZATION NAME AND ADDRESS Quantum Physics Division U.S. Bureau of Standards Boulder, CO 80303	10. PROGRAM ELEMENT, PROJECT, TASK AREA & WORK UNIT NUMBERS 54853 2301S208	
11. CONTROLLING OFFICE NAME AND ADDRESS Aero Propulsion Laboratory (AFWAL/POOC) Air Force Wright Aeronautical Laboratories Wright-Patterson AFB, OH 45433	12. REPORT DATE May 1981	
14. MONITORING AGENCY NAME & ADDRESS (if different from Controlling Office)	13. NUMBER OF PAGES 33	
16. DISTRIBUTION STATEMENT (of this Report)  Approved for public release; distribution unlimited		15. SECURITY CLASS (of this report) Unclassified
17. DISTRIBUTION STATEMENT (of the abstract entered in Block 20, if different from Report)		
18. SUPPLEMENTARY NOTES		
19. KEY WORDS (Continue on reverse side if necessary and identify by block number) oxygen, argon, metastable, electrons, radiation, quenching, excitation coefficient <i>1.1 et al.</i>		
20. ABSTRACT (Continue on reverse side if necessary and identify by block number) Measurements have been made of electron excitation coefficients for the $\alpha^1 A_g$ metastable state of $O_2$ . The measurements were made in mixtures 1 and 5% $O_2$ in Ar for mean electron energies between about 0.9 and 4 eV. The measured excitation coefficients are about 30% above predictions for 1% $O_2$ and about 30% below predictions for 5% $O_2$ . The measured rate coefficient for quenching of the $O_2(\alpha^1 A_g)$ state by O <sub>2</sub> is in good agreement with the literature value, but the rate coefficient for quenching by Ar is about twice previously published values.		

## PREFACE

This work was performed in the Quantum Physics Division, U.S. Bureau of Standards, at the Joint Institute for Laboratory Astrophysics under MIPR FY1455-80-00607. Dr. Tachibana was at the Joint Institute for Laboratory Astrophysics while on leave from the Department of Electronics, Kyoto Technical University, Kyoto, Japan. This work was performed during the period October 1979 through September 1980 under Project 2301 Task S2, "Plasma Research, Gas Discharge and Laser Plasmas." The Air Force contract manager was Dr. Alan Garscadden, Energy Conversion Branch, Aero Propulsion Laboratory.

Accession For	
NTIS GRA&T	<input checked="" type="checkbox"/>
DTIC TAB	<input type="checkbox"/>
Unpublished	<input type="checkbox"/>
Justification	
Py.	
Instrumentation	
Avail. for Reproduction	
Comments	

A

TABLE OF CONTENTS

<u>Section</u>	<u>Page</u>
I. INTRODUCTION . . . . .	1
II. EXPERIMENTAL APPARATUS AND PROCEDURE . . . . .	3
III. QUENCHING RATE COEFFICIENTS. . . . .	15
IV. EXCITATION COEFFICIENTS. . . . .	20
V. CONCLUSIONS. . . . .	25
REFERENCES . . . . .	27

## LIST OF ILLUSTRATIONS

<u>Figure</u>	<u>Page</u>
1. Schematic of Experiment. . . . .	4
2. Detailed Schematic of Apparatus. . . . .	7
3. Detector Response to Square Wave IR Signal . . . . .	8
4. AC Mode of Detector Operation. . . . .	10
5. Compensated or "DC" Mode of Detector Operation . . . . .	11
6. Representative Detector Output . . . . .	12
7. Example of Processed Data and of Fits of Exponential Rise and Fall. . . . .	13
8. $O_2(\alpha/\Lambda)$ Decay Constant vs Total Gas Density. . . . .	17
9. Determination of Quenching and Diffusion Coefficients. . .	18
10. Gas Density Dependence of $\alpha/N$ Values . . . . .	21
11. Experimental and Calculated $\alpha/N$ Values for 1% $O_2$ -99% Ar. .	22
12. Experimental and Calculated $\alpha/N$ Values for 5% $O_2$ -95% Ar. .	23

## LIST OF TABLES

SECTION I  
INTRODUCTION

The metastable states of  $O_2$  such as  $a^1\Delta_g$  and  $b^1\Sigma_g^+$  have important roles not only in the earth's atmosphere but also in lasers of the excitation-energy transfer type, e.g., the  $O_2$ -iodine molecular laser. A previous paper<sup>1</sup> (hereafter referred as I) reported a measurement of the coefficients for electron excitation of the  $b^1\Sigma_g^+$  state as a function of the ratio of the electric field to the gas density E/N using a drift tube technique. At that time it was not possible to measure the excitation coefficients for the  $a^1\Delta_g$  state mainly because of the extremely small radiative transition probability of the state and the lack of a high sensitivity and low noise detector for the  $1.27 \mu m$  radiation emitted in the (0-0) band of the  $a^1\Delta_g - X^3\Sigma_g^-$  transition. In the meantime, we have been able to purchase a suitable IR detector and have used it to measure the rate coefficients for the  $O_2(a^1\Delta)$  state.

The experimental measurement and subsequent analysis of electron excitation coefficients for the  $O_2(a^1\Delta_g)$  state is an important step in the development of one's ability to use collision cross section data to predict and optimize the operation of electrical discharges in gas mixtures containing oxygen. There is fair agreement among the determinations of the cross section for direct excitation of the  $O_2(a^1\Delta_g)$  state by electron beam techniques.<sup>2</sup> Therefore, the objectives of these measurements are to test these cross sections for swarm or discharge conditions, to measure the contribution of cascading to the  $O_2(a^1\Delta_g)$  state excitation, and to determine experimentally the relative importance of competing excitation processes such as vibrational excitation. Throughout the analyses of this data, we must look for clues as to the source of the large discrepancy between measured and predicted excitation coefficients

for the  $O_2(b^1\Sigma_g^+)$  state which were found by Lawton and Phelps<sup>1</sup> and attributed to an unexpected cascading from the higher metastable states, e.g., the  $c^1\Sigma_u^-$  state.

Most of the theory of the experiment and procedure given in I can be used in this experiment. We, therefore, summarize very briefly in Section II the equations relating the observed signal to the excitation coefficient.

Somewhat more detailed descriptions are given in Section II for the differences in the experiments caused by differences in the detectors.

The rate coefficients for quenching of the  $a^1\Delta_g$  state by  $O_2$  and by Ar are given in Section III. In Section IV the excitation rate coefficients for the state are given as a function of E/N and are compared with the theoretical predictions.

SECTION II  
EXPERIMENTAL TECHNIQUE

A schematic of the drift tube technique used for determination of excitation coefficients for the  $O_2(a^1\Delta_g)$  state is shown in Fig. 1. A continuously operating 100 W high pressure mercury lamp is passed through broad band interference filters centered at 190 nm (not shown) and then through a quartz window coated on the inside with a semi-transparent cathode film of evaporated Pd-Au. The resulting photoelectrons enter the gas filled, parallel plate drift tube. The anode voltage is modulated so as to periodically apply a known electric field  $E$  and so produce electrons with a modulated mean energy. These electrons may excite the  $O_2$  molecules to the  $a^1\Delta_g$  state. Since the radiative lifetime of these metastables is very long (3900 sec), most of the metastables will be destroyed by diffusion to the drift tube electrodes or by collisional quenching by the  $O_2$  molecules or by the Ar atoms used to reduce the diffusion loss. At best, about one molecule in 2000 is able to radiate at 1.27  $\mu\text{m}$ .

A very brief outline of the theory relating the radiated power  $P$  at 1.27  $\mu\text{m}$  reaching the detector from the drift tube is given next. Thus, the power is given by

$$P = h\nu A \frac{\Omega}{4\pi} \int_V \eta[a] dV , \quad (1)$$

where  $h\nu$  is the photon energy,  $A$  is the measured radiative transition probability<sup>3</sup> as corrected for collision induced radiation by the Ar buffer gas,<sup>4</sup>  $\Omega$  is the solid angle of the detector as seen from the center of the drift tube and  $\eta$  is the efficiency of photon collection from various parts of the drift tube relative to that at the center. The density of  $O_2(a^1\Delta_g)$  metastables  $[a]$  is obtained from the solution of the continuity equation

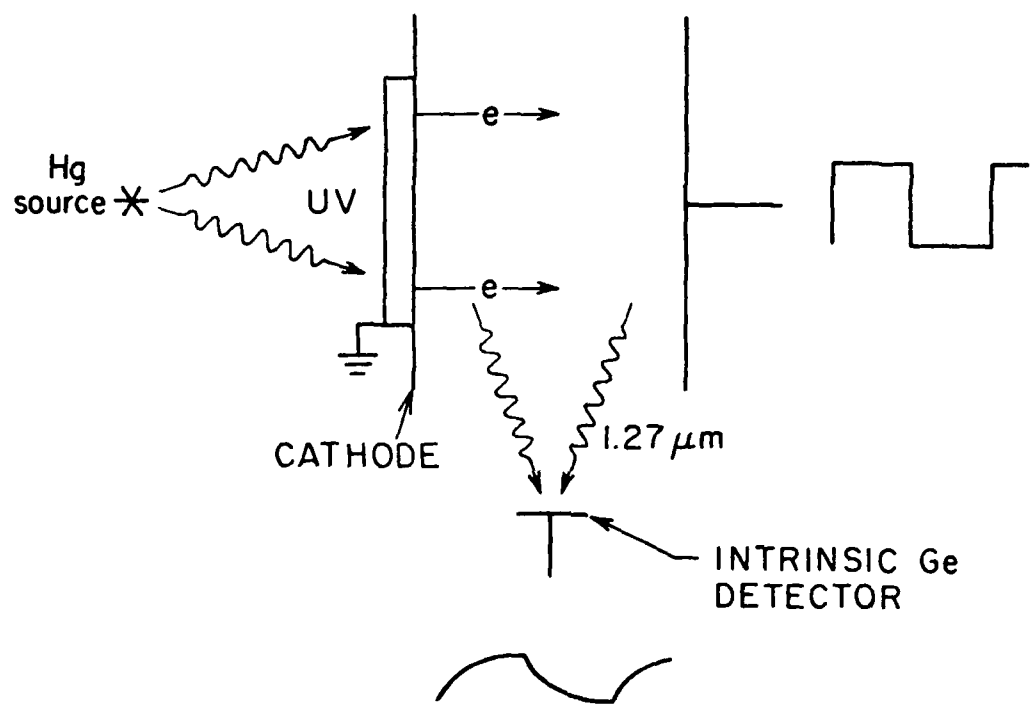


Figure 1. Schematic of Experiment.

$$\frac{[a]}{[t]} = DV^2 [a] - (k_d N + A) [a] + k_e N n_e , \quad (2)$$

where  $D$  is the effective metastable diffusion coefficient,  $k_d$  is the effective rate coefficient for metastable destruction by  $O_2$  and by Ar at the total gas density  $N$ , and  $n_e$  is the electron density  $n_e$ . Here the electron excitation rate coefficient  $k_e$  is given by

$$k_e = \int_0^\infty v Q_a(\varepsilon) \varepsilon^{1/2} f(\varepsilon) d\varepsilon , \quad (3)$$

where  $v$  and  $\varepsilon$  are the electron speed and energy,  $Q_a(\varepsilon)$  is the cross section for electron excitation of the  $O_2(a^1 \Delta_g)$  state, and  $f(\varepsilon)$  is the normalized electron energy distribution. Here we assume that any excitation of the  $O_2(a^1 \Delta_g)$  state by cascading from higher excited states is rapid on the time scale of these experiments and is included in  $k_e$ .

The coefficients describing the destruction of metastables in this experiment are determined from measurements of the time dependence of the 1.27  $\mu m$  emission. The diffusion term in Eq. (2) adds greatly to the difficulty of quantitative analysis of the emission data and the reader is referred to 1 for a detailed discussion. For the present purposes we will limit the discussion to high gas densities where

$$\gamma = k_d N \gg A + D(\pi/L)^2 , \quad (4)$$

where  $L$  is the distance between the drift tube electrodes. In this limit the metastable density is given by

$$[a] \approx \frac{k_e N n_e}{\gamma} (1 - e^{-\gamma t}) = \frac{e j_e}{e \gamma} (1 - e^{-\gamma t}) , \quad (5)$$

where  $k_e N = \omega_e w_e$  and  $e$ ,  $w_e$  and  $j_e$  are the electron charge, drift velocity and current density. The radiated power reaching the detector from the drift tube reaches its maximum value  $P_{max}$  when  $\gamma t \gg 1$  and is given by

$$P_{\max} = \frac{hvA}{e} \frac{xL}{\gamma} \frac{G}{q} i , \quad (6)$$

where  $i$  is the total current through the drift tube and  $G$  and  $q$  are geometrical and current correction factors defined in I.

The drift tube shown in the detailed schematic of Fig. 2 is the same as the one used in I. The electrode spacing was 38.4 mm and the cathode area was  $0.28 \text{ m}^2$ . The period of the zero-based square wave anode voltage was varied from 10 to 25 sec depending on the decay constant of the  $a_g^{1\Delta}$  state. This data recording period was followed by a dead time of 15 sec for the computer processing as described below. The accelerating voltage ranged from 111 to 1152 V and the total current in the on-period was 0.02 to  $0.09 \mu\text{A}$ .

Measurements were made with 0.1 to 5%  $\text{O}_2$  in Ar at the total gas densities of  $10^{24}$  to  $2 \times 10^{25} \text{ m}^{-3}$ . The reason for using dilute  $\text{O}_2$  in Ar at relatively high pressure is that we expected to increase the detection efficiency of  $1.27 \mu\text{m}$  radiation by decreasing the non-radiative losses of  $a_g^{1\Delta}$  states due to the diffusion, i.e., by using Ar it is possible to reduce the  $\text{O}_2$  density and resultant quenching by a factor of ten. After  $\text{O}_2$  of 99.99% specified purity was bled into the drift tube from a liquid- $\text{N}_2$  cooled reservoir, Ar of 99.999% purity was bled into the tube directly from a high pressure cylinder.

A liquid- $\text{N}_2$  cooled intrinsic germanium detector (North Coast Model 403L) was mounted at the top of the drift tube. The specified responsivity and NEP (noise equivalent power) of the detector are  $7 \times 10^9 \text{ V/W}$  and  $1 \times 10^{-15} \text{ W Hz}^{-1/2}$  at  $1.3 \mu\text{m}$ . The typical "DC response" for a squarewave IR input signal, the width of which is comparable to the real signal, is shown in Fig. 3.

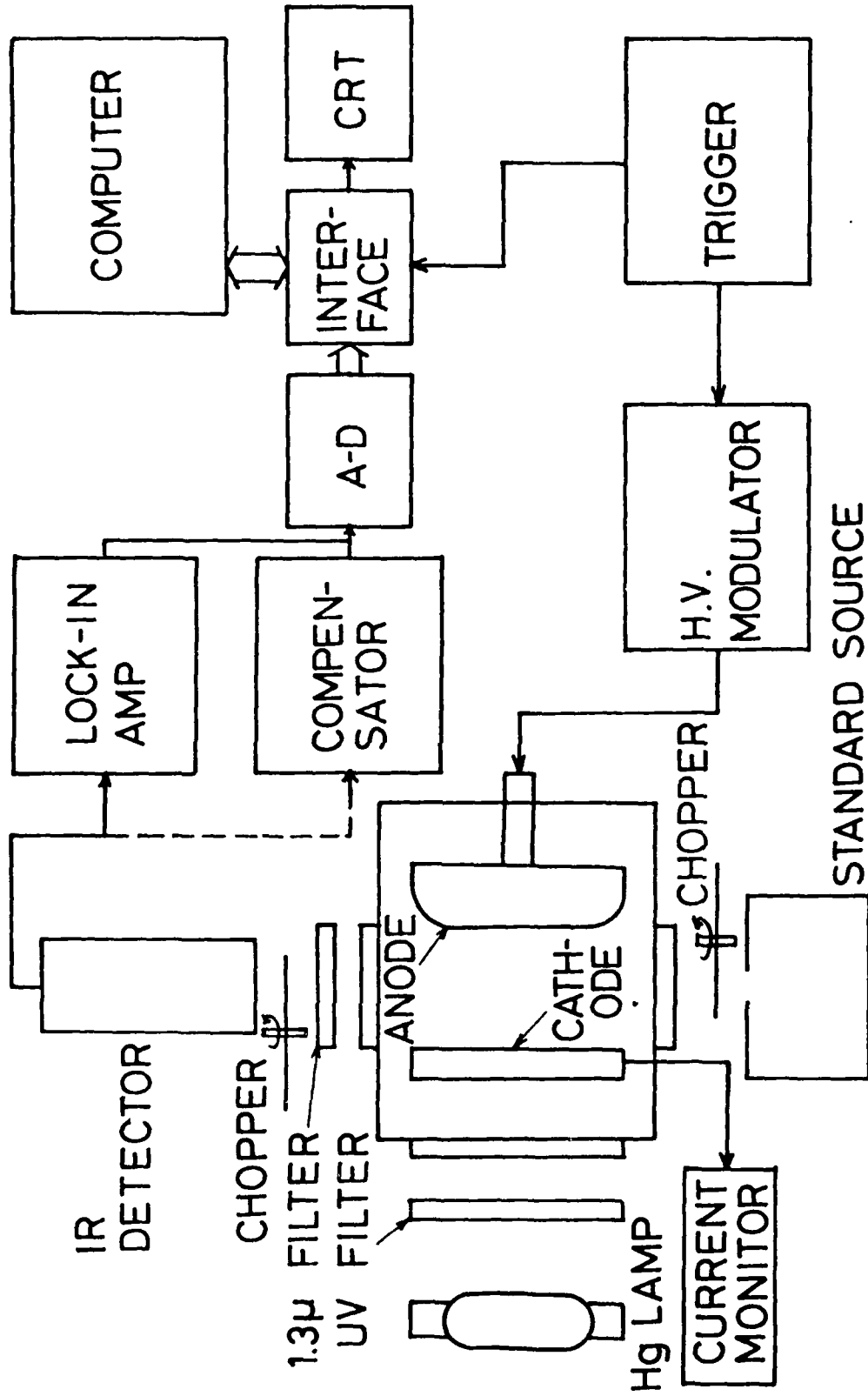


Figure 2. Detailed Schematic of Apparatus.

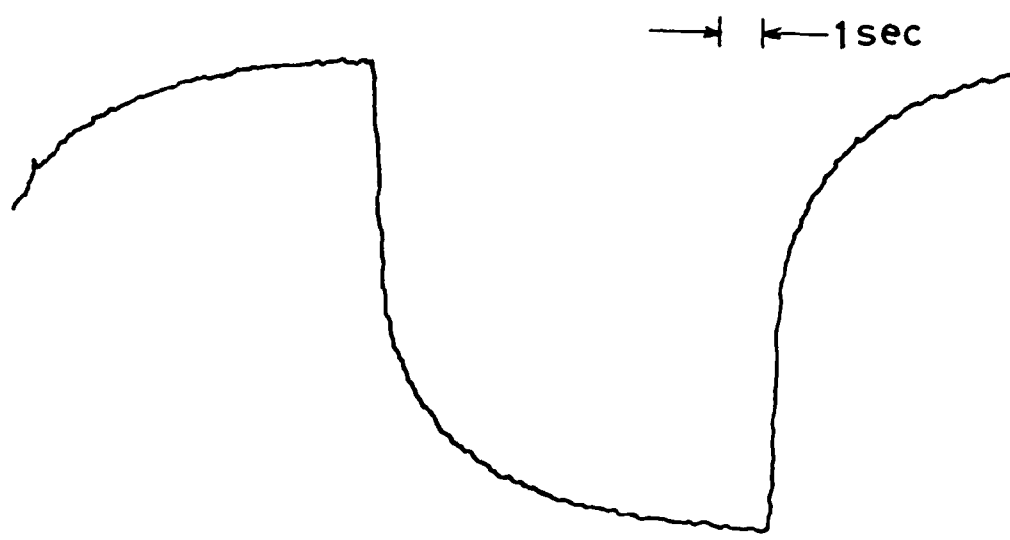


Figure 3. Detector Response to Square Wave IR Signal.

The response consists of fast and slow components, the time constants of which were about 10 msec and 3 sec, respectively. Two techniques have been used to overcome this problem. One way is to use only the fast response part by chopping the signal in front of the detector at a frequency of about 100 Hz and detecting the output signal through a lock-in amplifier. This method is referred to as AC-method hereafter and is shown schematically in Fig. 4. The other way is to use an amplifier which compensates for the 3 sec response and partially compensates for the 10 msec response. This was possible with a circuit as shown in Fig. 5.

Figure 5 also shows the current waveforms at the points indicated. This is a kind of feed-forward compensation and referred to as compensated DC-method hereafter. A merit of the DC-method is that we were able to get a higher S/N ratio and responsivity than with the AC-method, i.e., a factor of more than 2. A demerit is a rather critical adjustment of the compensation. However, we were able to check the compensation in the compensated DC-method using the AC-method at higher signal levels.

We encountered another problem due to spikes caused by cosmic rays, the heights of which were 5 to 20 mV at the output of the detector preamplifier. A representative AC-method signal from the detector is shown in Fig. 6. The width of a spike was usually only one sampling interval of the data recording system used, so that we were able to reject the spikes by a computer algorithm which replaced a sudden change in signal i.e., a spike, with the average value of the signal in adjacent channels.

A mini-computer was used as a data acquisition and analyzing system. The signal for the compensated amplifier or the lock-in amplifier was sampled every 40 to 200 msec depending upon the period of the anode voltage.

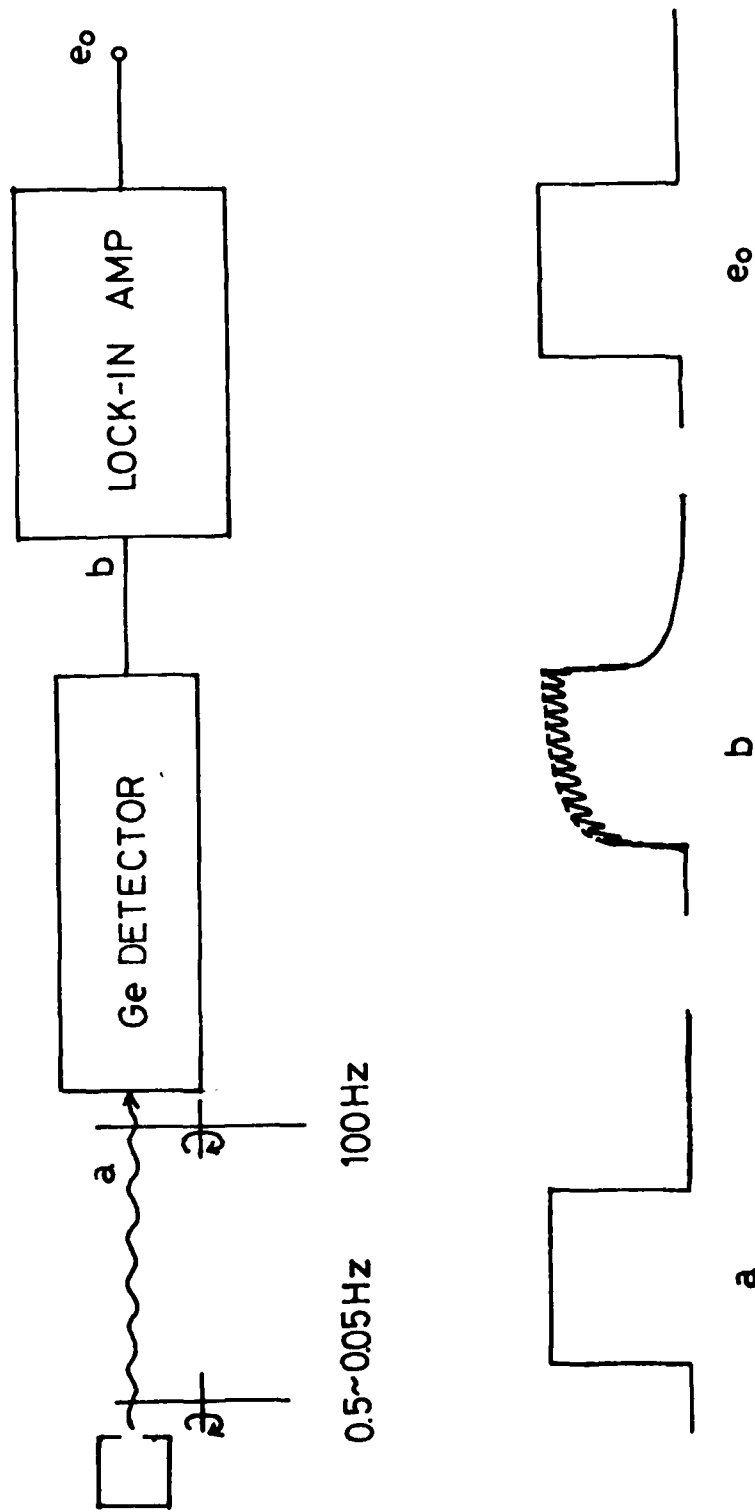


Figure 4. AC Mode of Detector Operation.

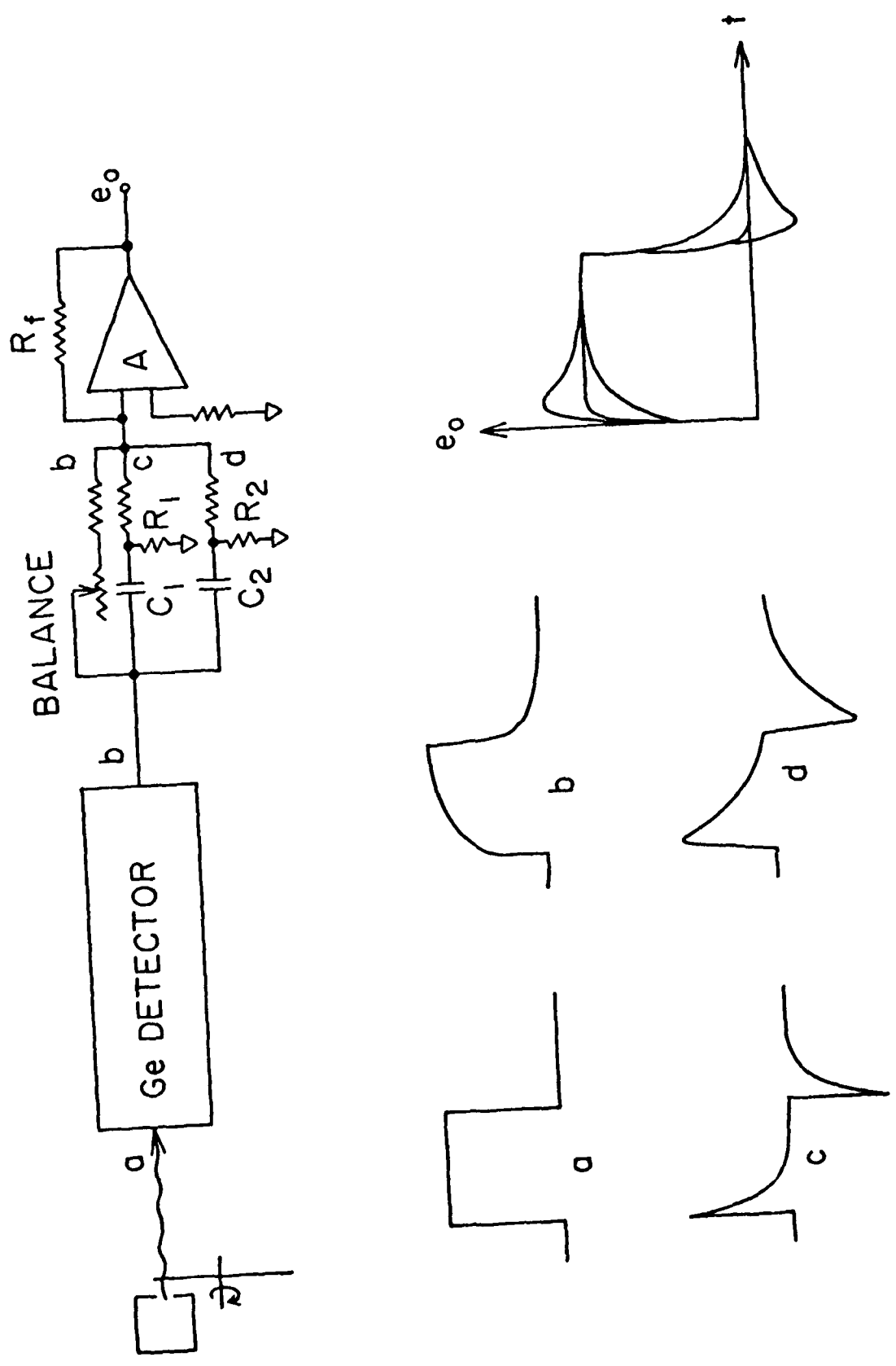


Figure 5. Compensated or "DC" Mode of Detector Operation.

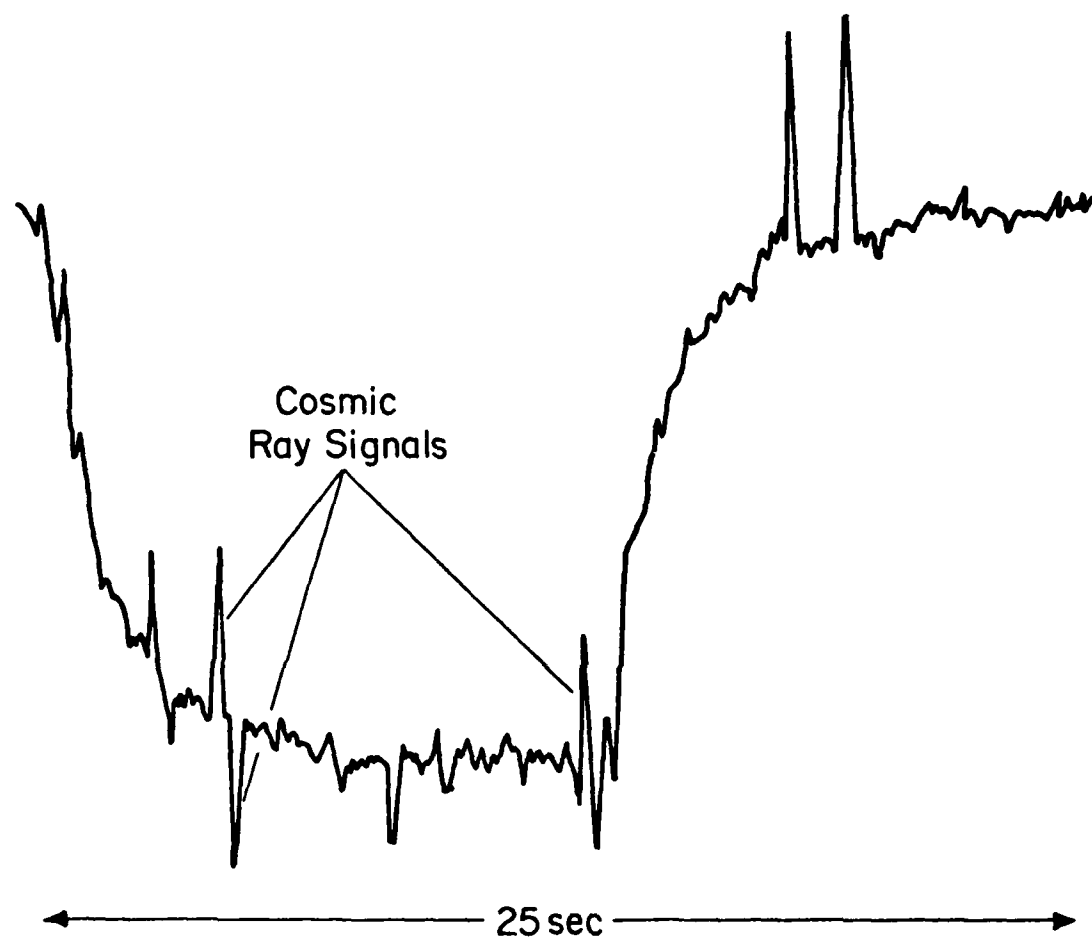


Figure 6. Representative Detector Output.

A set of data (256 points during a sweep) was stored in the computer and then analyzed to reject spikes due to cosmic rays. Sets of data were additively accumulated in the computer memory. After a desired number of sweeps (8-22) were completed, data was stored on a magnetic tape. The computer was also used to analyze the data by a least squares fitting procedure, and the data points as well as the fitted results were displayed on a CRT.

The (0-0) band of the  $a^1\Delta_g - X^3\Sigma_g^+$  system at  $1.27 \mu\text{m}$  was isolated from the background radiation by an interference filter with 75% peak transmission at  $1.32 \mu\text{m}$  and a  $0.147 \mu\text{m}$  FWHM. The value  $\langle f_i \rangle$  defined by Eq. (6) in I was calculated using the emission band profile of Wood et al.<sup>5</sup> Although the necessary data on vibrational relaxation of the  $v=1$  level of  $O_2(a^1\Delta)$  to the  $v=0$  level is not available,<sup>5</sup> the near coincidence of wavelengths and transition probabilities for the 0-0 and 1-1 transitions<sup>7</sup> means that our measurements are independent of the ratio of populations in the  $v=1$  and  $v=0$  levels of the  $O_2(a^1\Delta)$  state.

The calibration of the detection system was done with a black-body light source mounted on the opposite side of the drift tube from the detector. An aperture of 1.50 mm diameter was placed in front of the source 0.47 m from the detector so as to reduce the black-body signal. When the temperature of the source was  $213^\circ\text{C}$  the intensity at the detector was comparable to that observed for the  $O_2(a^1\Delta_g)$  emission. A chopper in front of the source modulated the black-body emission at a period of 20 sec, which was also comparable to that used for the  $a^1\Delta_g$  emission.

The spatial variation of the detection efficiency was measured by a method similar to that described in I. A hollow sphere with a small aperture

covered by a diffuser was scanned over the drift region. The sphere was illuminated by a iodine-tungsten lamp through a quartz light pipe. The results show that the radially averaged detection efficiency  $\eta(z)$  is given by

$$\eta(z) = 0.973 + 0.05 \sin(2\pi z/L) - 0.23(1-2z/L) . \quad (7)$$

The geometrical factor  $G$  is therefore given by

$$G = 0.973 G_A + 0.05 G_B - 0.23 G_C , \quad (8)$$

where  $G_A$  and  $G_C$  are the same as given in I.  $G_B$  is given by

$$G_B = \frac{2\pi a}{[a^2 + (2\pi)^2]^2} \frac{(d^2 + \pi^2)}{[d^2 + (2\pi)^2]} , \quad (9)$$

instead of Eq. (A1) in I. Here  $d^2 = k_d N L^2 / D$ .

SECTION III  
QUENCHING RATE COEFFICIENTS

Figure 7 shows a typical  $1.27 \mu\text{m}$  signal as a function of time. The solid curves show the least squares fits to the data of functions of the form  $a_1 + a_2 \exp(-a_3 t)$ . The average value  $\gamma$  of the exponents obtained from rise and fall parts was assumed equal to the decay constant for the fundamental diffusion mode as in I. The decay constant  $\gamma$  is plotted versus the total gas density  $N$  for various  $\text{O}_2$ -Ar mixtures in Fig. 8. The data points measured by the compensated DC-method, shown by circles are consistent with the points measured by the AC-method, shown by triangles. The radiative transition probability  $A$  for the  $1.27 \mu\text{m}$  band is much smaller than  $\gamma$ , so that

$$\gamma = \pi^2 D/L^2 + k_d N_T . \quad (10)$$

Here the effective quenching rate coefficient  $k_d$  is given by  $k_d^0 = (k_d [\text{O}_2] + k_d^A [\text{Ar}])/([\text{O}_2] + [\text{Ar}])$ , where  $k_d^0$  and  $k_d^A$  are the quenching rate coefficients by  $\text{O}_2$  and by Ar, respectively. In order to obtain  $D$  and  $k_d$ , we use a plot of  $\gamma N$  vs  $N^2$ . In this plot  $D$  is obtained from the intercept and  $k_d$  from the slope. This plot is shown in Fig. 9 for  $\text{O}_2$  fractional concentrations of 1 and 5%. Circles and triangles are the same as for Fig. 8 and bars show the peak to peak errors. Both lines give the same intercept, from which the diffusion coefficient is determined to be  $D_N = (2.8 \pm 0.2) \times 10^{20} \text{ m}^{-1} \text{ sec}^{-1}$ . This value is smaller than the value  $4.9 \times 10^{20} \text{ m}^{-1} \text{ sec}^{-1}$  for pure  $\text{O}_2$  measured by Vidaud, et al.<sup>8</sup> We can determine  $k_d^0$  and  $k_d^A$  from the two  $k_d$  values at different  $\text{O}_2$  contents to be  $k_d^0 = (1.67 \pm 0.1) \times 10^{-24} \text{ m}^3 \text{ sec}^{-1}$  and  $k_d^A = (1.8 \pm 0.1) \times 10^{-25} \text{ m}^3 \text{ sec}^{-1}$ . As seen in Table 1, the value for  $k_d^0$  agrees well with some of the recent measurements. However, the value for  $k_d^A$  is larger than recent measurements by about a factor of two. Because of the very small value of  $k_d^A$  and the high Ar densities used we are concerned that impurities may cause a significant error in our result.

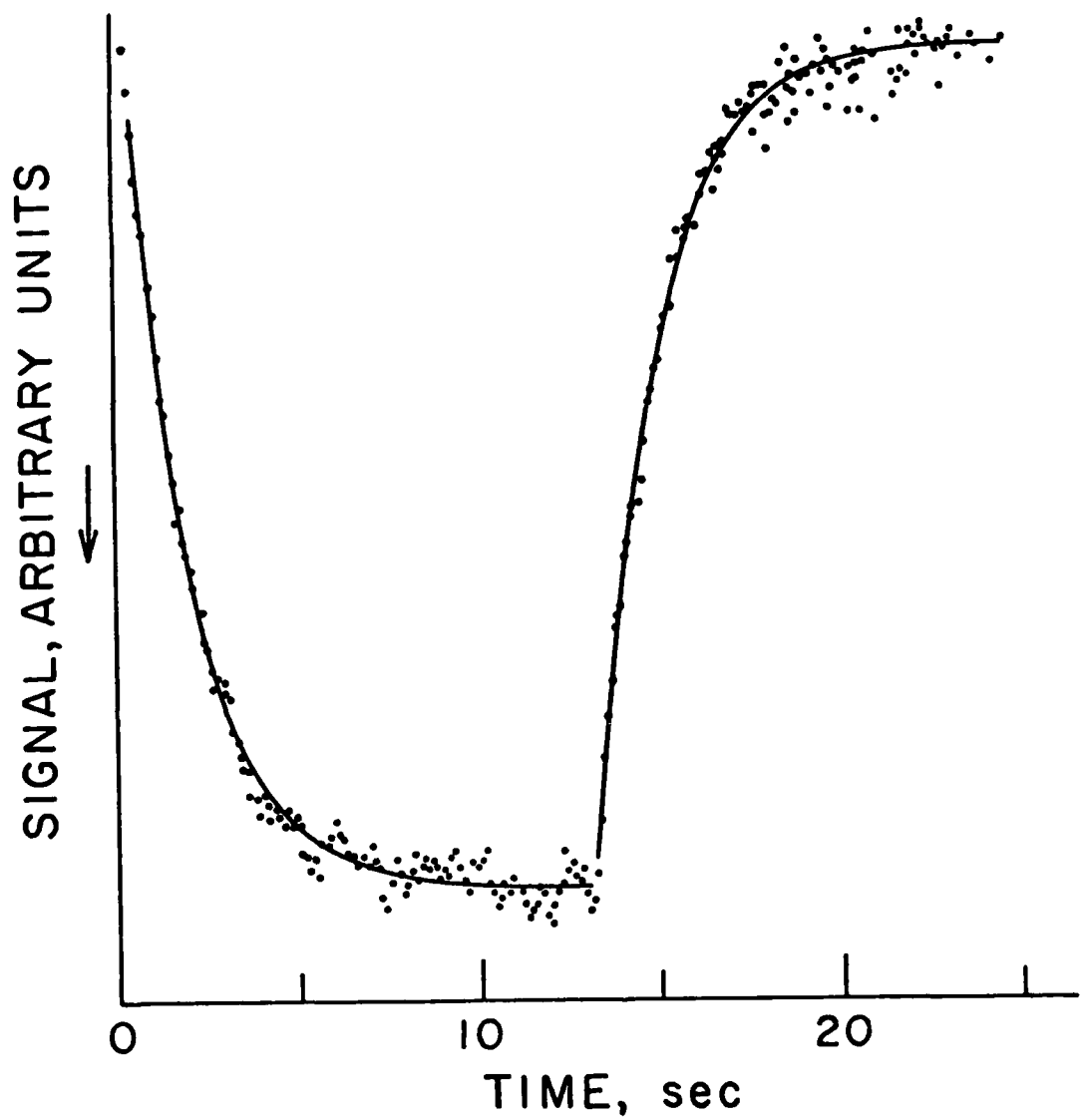


Figure 7. Example of Processed Data and of Fits of Exponential Rise and Fall.

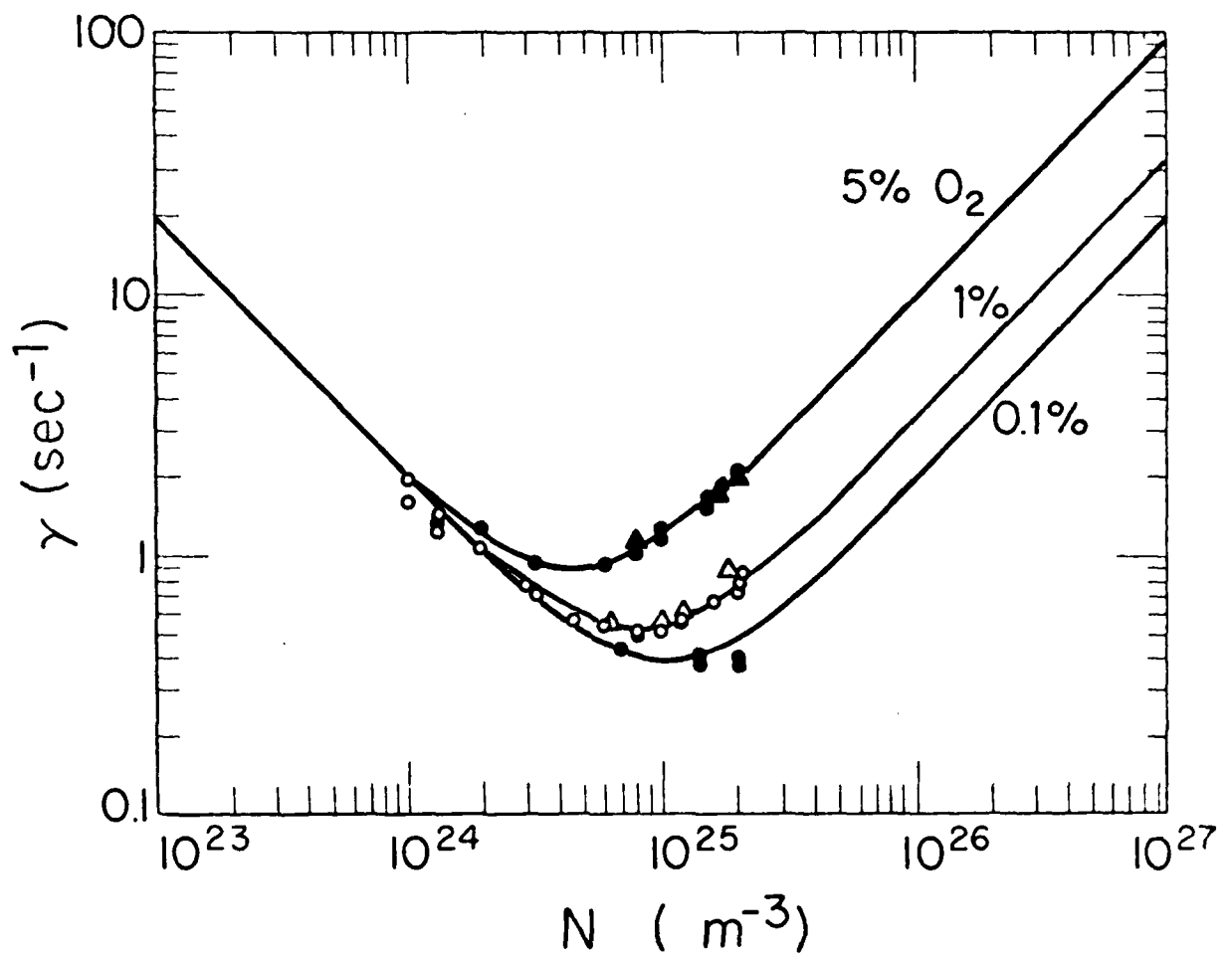


Figure 8.  $O_3(a^1\Delta)$  Decay Constant vs Total Gas Density.

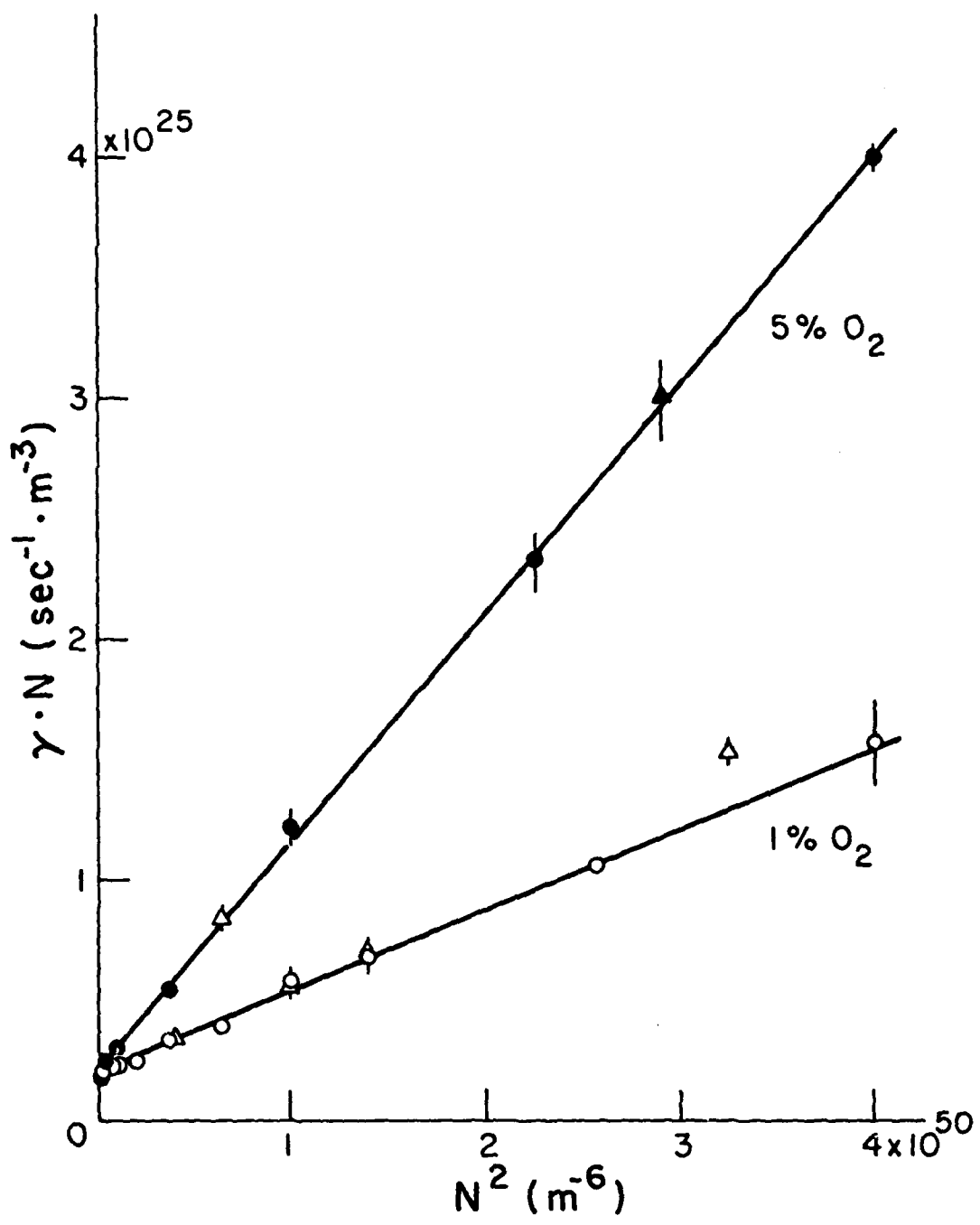


Figure 9. Determination of Quenching and Diffusion Coefficients.

TABLE 1

RATE CONSTANTS FOR QUENCHING OF  $O_2(a^1\Delta_g)$  BY VARIOUS GASES\*

quencher	this work	Ref. 9	Ref. 10	Ref. 11	Ref. 12	Ref. 13	Ref. 14	Ref. 15
$O_2$	1.57	1.47	1.56		1.7	2.22	2.4	2.04
$N_2$				0.14	$\leq 0.01$	$< 0.003$	$\leq 0.11$	0.042
$H_2$		4.15		5.3	3.7	4.53		
$CO_2$		$\leq 0.013$			0.08	0.015	3.9	
He				0.008	0.01	$< 0.008$		
Ar	0.018			0.009	0.01	$< 0.008$	$\leq 0.21$	
Kr				0.0079				
Xe				0.034				

\* in units of  $10^{-18} \text{ cm}^3/\text{sec.}$ .

SECTION IV  
EXCITATION COEFFICIENTS

Figure 10 shows the excitation coefficients  $\alpha/N$  as a function of  $N$  for a mixture of 1%  $O_2$  and 99% Ar for two values of  $E/N$ . The solid circles were calculated using a refined form of Eq. (10), actually Eq. (17) in I, with  $q=1$ ,  $G=1$  and  $A = 2.58 \times 10^{-4} \text{ sec}^{-1}$ . The solid triangles show the data corrected by the appropriately calculated values of  $G$  and by the factor due to the effect of collision-induced transitions, that is,  $\bar{A}/A = 1 + 0.258 \rho_A + 3.58 \rho_O$ . Here  $\bar{A}$  is the effective radiative transition probability and  $\rho_A$  and  $\rho_O$  are the densities of  $O_2$  and Ar in units of  $2.69 \times 10^{25} \text{ atom/m}^3$ . The factor for  $\rho_O$  is taken from Ref. 3 and that for  $\rho_A$  from Ref. 4, respectively. The open circles show the final results corrected by the  $q$  values calculated from Eq. (14) in I. The  $q$ -correction amounted to a factor of from 1 to 7, depending on the  $E/N$  and  $N$  values. For our conditions the departure of  $q$  from unity was caused by electron attachment, i.e., ionization was negligible. The corrected results for the rate coefficients at a fixed  $E/N$  value are independent of  $N$  except for some points at the lower  $E/N$  and lower  $N$ . This indicates that the attachment coefficients used in the calculation of  $q$ -values were reasonable. The final results for  $\alpha/N$  are shown as a function of  $E/N$  in Figs. 11 and 12 for fractional  $O_2$  concentrations of 1 and 5%, respectively.

The main differences in the sources of experimental error in the present measurements and those of I are as follows: the radiative transition probability for the  $a^1\Delta_g$  state (~20%), least squares fitting of the waveform (10%), calibration using the black-body light source (10%) and the differences in the spectral sensitivity at  $1.27 \mu\text{m}$  and at  $1.35 \mu\text{m}$  where the convolution of

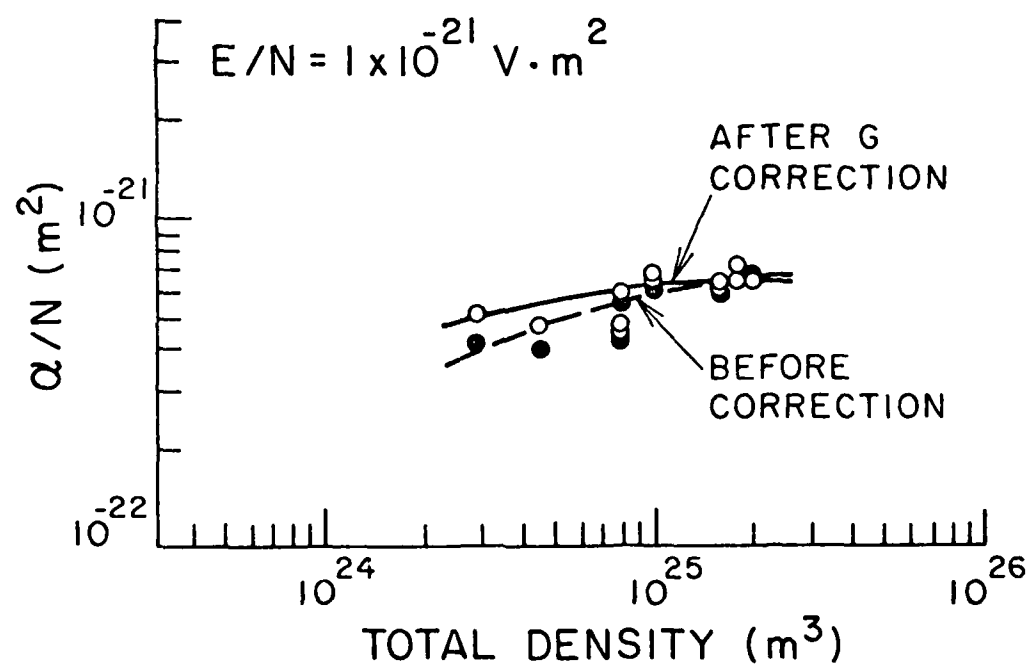
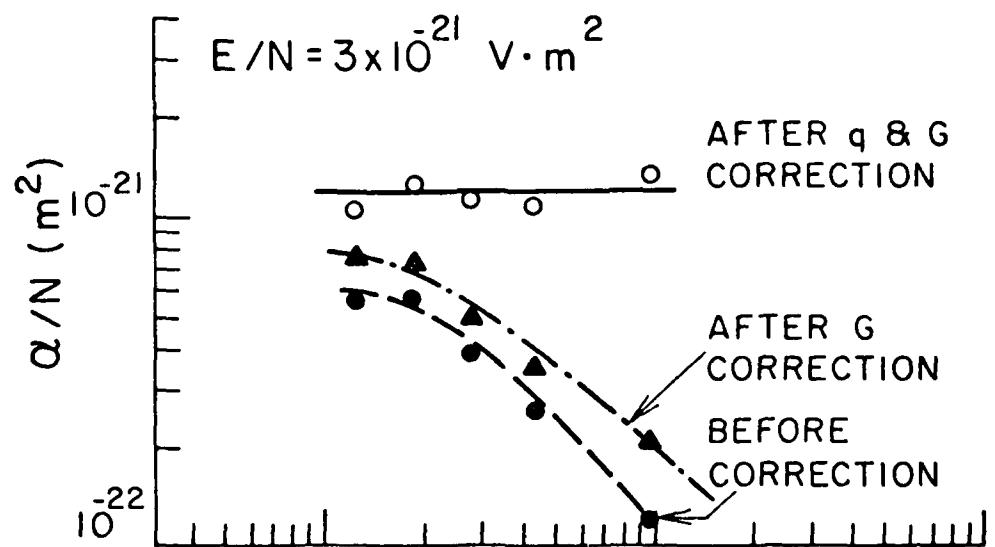


Figure 10. Gas Density Dependence of  $\alpha/N$  Values.

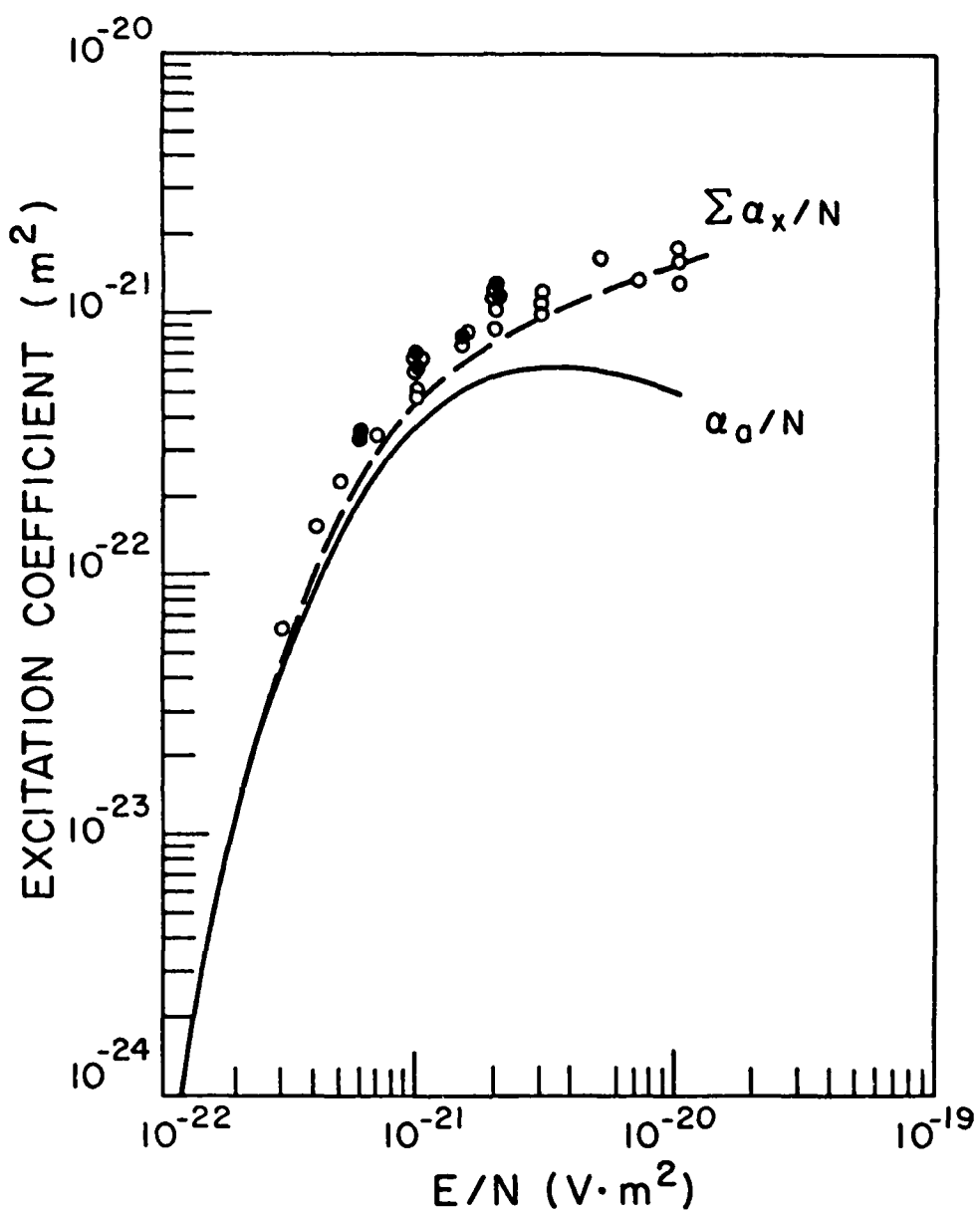


Figure 11. Experimental and Calculated  $\alpha/N$  Values for 1%  $O_2$ -99% Ar.

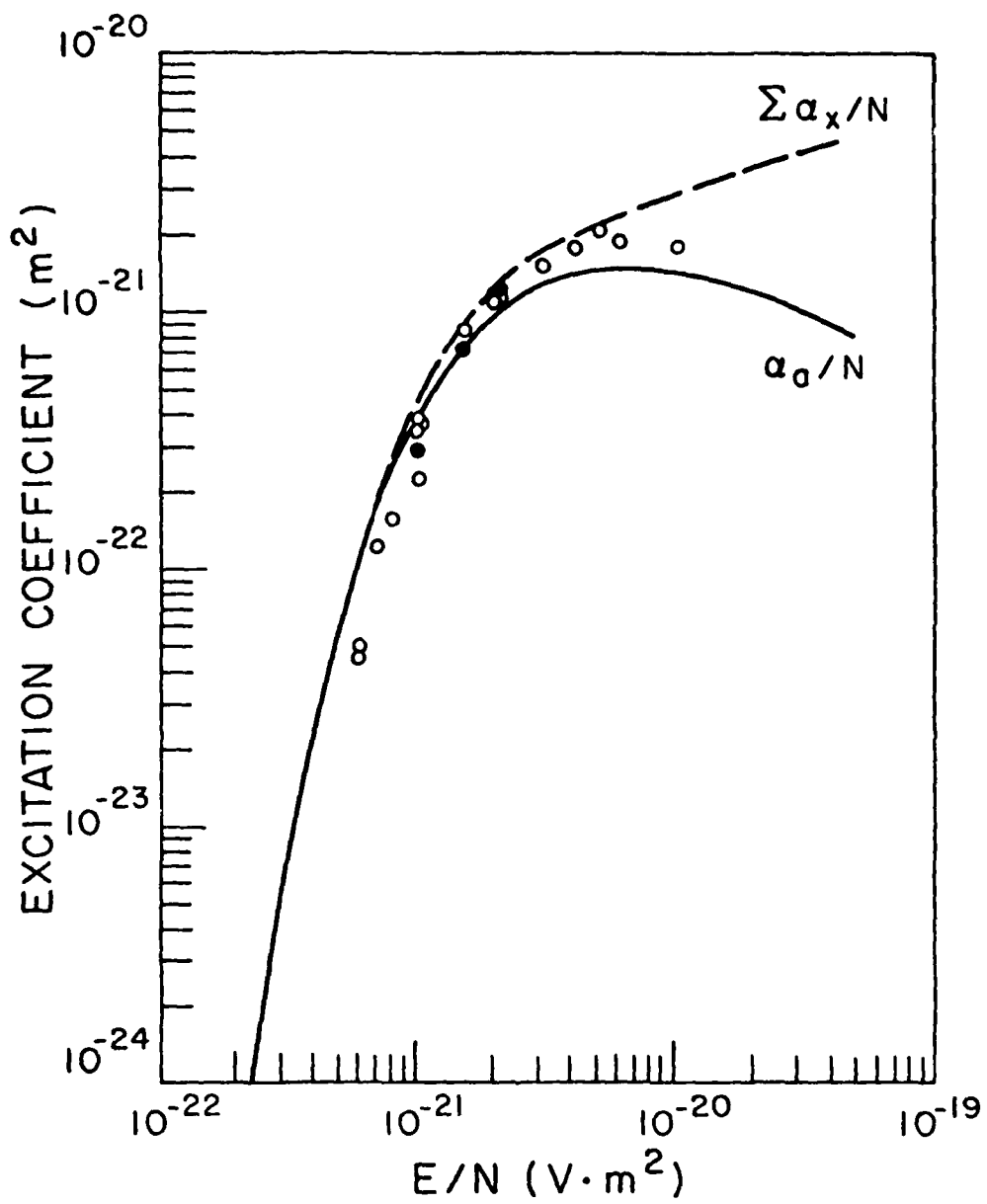


Figure 12. Experimental and Calculated  $\alpha/N$  Values for 5%  $O_2$ -95% Ar.

the transmittance of an IR-filter and the spectral intensity distribution of the black-body source has a maximum (5%). The total estimated uncertainty in  $\alpha/N$  is 33% in this case instead of 25% in I.

The calculated values of  $\alpha/N$  for direct excitation of the  $O_2(a^1\Delta_g)$  state are shown in Figs. 11 and 12 by the solid lines. The dashed lines show the calculated results when collisional cascading from higher lying states is included. The efficiency of the cascading was assumed to be 100% as in I. From Figs. 11 and 12 it is seen that the measured rate coefficients are slightly higher than the calculated values for the  $O_2$  concentrations of 1%, while the tendency reverses for 5%  $O_2$ , especially for lower E/N values. The measured results agree with the calculated values when the cascading contributions at higher E/N values are included. The cascading in our E/N range, however, is mainly from the  $b^1\Sigma_g^+$  state and its efficiency may be considered to be close to 100%.

SECTION V  
CONCLUSIONS

The measurement of electron excitation rate coefficients described in this report provides a crucial set of data in the development of the ability to predict the behavior of electrons in pure oxygen or oxygen mixed with other gases. Devices and systems utilizing electron motion in oxygen include the proposed gas discharge excited oxygen-iodine lasers, electron beam propagation in the earth's atmosphere, ozone generators, and air insulation systems. In particular, these experiments provide for the first time quantitative measurements of the rates of production of the  $O_2(a^1\Delta)$  metastable state under gas discharge-like conditions of mean electron energy and electron energy spread. Furthermore, these experiments show the usefulness of the drift tube technique for the measurement of excitation coefficients for metastable states which have very long radiative lifetimes and which radiate at infrared wavelengths where high sensitivity-low noise detectors are difficult to obtain and to operate.

The measured collisional deexcitation rate coefficient for  $O_2(a^1\Delta)$  metastables by  $O_2$  is in good agreement with published data. Our de-excitation rate coefficient for  $O_2(a^1\Delta)$  by Ar is about twice the literature value. This could indicate the presence of higher than expected concentrations of impurities in our Ar supply. A test of this hypothesis will be made when we use a new Ar tank. We have no plans to attempt purification of the Ar, since our primary objective is the determination of excitation rate coefficients and since the data analysis includes the measurement of the rate of metastable destruction for each set of data.

The measured excitation coefficients for  $O_2(a^1\Delta_g)$  excitation are within +30% of values calculated using our Boltzmann code and using our previously

recommended cross section sets for  $O_2$  and for the buffer gas, Ar. Thus, our present predictive capability for rates of excitation of the  $O_2(a^1\Delta)$  state is about  $\pm 30\%$ . We have no explanation for this systematic decrease in the ratio of measured to calculated excitation coefficients with increasing fractional oxygen concentration. Before undertaking a more extensive investigation of possible modifications of the electron collision cross section sets, we wish to extend the measurements of excitation coefficients to a wider range of fractional  $O_2$  concentrations and to higher E/N. The higher E/N and higher mean energy data is of particular importance to an evaluation of the role of  $O_2(a^1\Delta)$  excitation by cascading from higher excited states of  $O_2$ . The higher mean electron energies are of practical importance because they are representative of discharge conditions of higher electrical power input.

In addition to the measurements of excitation coefficients at higher E/N and over a wider range of ratios of  $O_2$  to Ar densities discussed previously, we recommend that:

- (a) measurements of the rate coefficients for vibrational excitation of ground states of  $O_2$  be made using, for example, the transfer of excitation from  $O_2$  to  $CS_2$  with subsequent emission at 6.5  $\mu\text{m}$ .
- (b) a search be made for evidence of electron excitation of the metastable Herzberg states of  $O_2$ , e.g., the  $c^1\Sigma$  state which emits very weakly at wavelengths near 500 nm.
- (c) measurements be made of the coefficients for dissociative excitation of  $O_2$  using, for example, absorption of the OI resonance lines near 130 nm. We have recently received notice of support for this project from another agency.

REFERENCES

1. S. A. Lawton and A. V. Phelps, J. Chem. Phys. 69, 1055 (1978).
2. S. Trajmar, D. C. Cartwright and W. Williams, Phys. Rev. A4, 1482 (1971); F. Linder and H. Schmidt, Z. Naturforsch. 26a, 1617 (1971); R. I. Hall and S. Trajmar, J. Phys. B8, L293 (1975); K. Wakiya, J. Phys. B11, 3931 (1978).
3. R. M. Badger, A. C. Wright, and R. F. Whitlock, J. Chem. Phys. 43, 4345 (1965).
4. C. W. Cho, E. J. Allin, and H. L. Welsch, Canad. J. Phys. 41, 1991 (1963).
5. H. C. Wood, W.F.J. Evans, E. J. Llewellyn, and A. V. Jones, Canad. J. Phys. 48, 862 (1970).
6. R. J. Collins and D. Husain, J. Photochem. 1, 481 (1962/73); J. G. Parker, J. Chem. Phys. 62, 2235 (1975); P. M. Borrell, P. Borrell, and K. R. Grant, JCS Faraday II 76, 923 (1980).
7. P. H. Krupenie, J. Phys. Chem. Ref. Data 1, 423 (1972).
8. P. H. Vidaud, R. P. Wayne, and M. Yaron, Chem. Phys. Lett. 38, 306 (1976).
9. A. Leiss, U. Schurath, K. H. Becker, and E. H. Fink, J. Photochem. 8, 211 (1978).
10. P. Borrell, P. M. Borrell, and M. D. Pedley, Chem. Phys. Lett. 31, 300 (1977).
11. R. J. Collins, D. Husain and R. J. Donovan, J. Chem. Soc. Farad. Trans. II 69, 145 (1973).
12. K. H. Becker, W. Groth, and U. Schurath, Chem. Phys. Lett. 8, 259 (1971).
13. F. D. Findlay and D. R. Snelling, J. Chem. Phys. 55, 545 (1971).
14. I. D. Clark and R. P. Wayne, Chem. Phys. Lett. 3, 93 (1969).
15. R. P. Steer, R. A. Ackerman, and J. N. Pitts, Jr., J. Chem. Phys. 51, 843 (1969).

END  
DATE  
FILMED

9 28 1981

DTIC